# Structural Characterization of Solar Cell Prototypes Based on Nanocrystalline $TiO_2$ Anatase Sensitized with Ru Complexes. X-ray Diffraction, XPS, and XAFS Spectroscopy Study

Y. V. Zubavichus,[†] Yu. L. Slovokhotov,[†] M. K. Nazeeruddin,[‡] S. M. Zakeeruddin,[‡] M. Grätzel,[‡] and V. Shklover*[,§]

*Laboratory of Polymer Structural Studies, Institute of Organoelement Compounds, Russian Academy of Sciences, 28 Vavilov St., Moscow 117813, Russia, Laboratory of Photonics and Interfaces, Institute of Physical Chemistry, Swiss Federal Institute of Technology, CH-105 Lausanne, Switzerland, and Laboratory of Crystallography, Swiss Federal Institute of Technology, CH-8092 Zürich, Switzerland*

*Received February 15, 2002. Revised Manuscript Received June 8, 2002*

Prototype solar cells made up of nanocrystalline anatase supported on a conducting glass and sensitized with two $Ru^{2+}$ complexes (*cis*-dithiocyanatobis(2,2′-bipyridine-4,4′-dicarboxylate)ruthenium(II), or red dye, and (4,4′,4″-tricarboxy-2,2′:6′,2″-terpyridine)ruthenium(II), or black dye) are characterized with out-of-plane X-ray diffraction, X-ray photoelectron spectroscopy, and Ti K-edge XAFS (XANES and EXAFS), as well as by powder X-ray diffraction of the pure dyes used for a coating of a $TiO_2$ layer. The data indicate, within the sensitivity limits of the methods applied, that the dyes most probably form (partial coverage) a monolayer at the surface of anatase nanoparticles. Coating with the dyes leads to a stronger distortion of the local environment of Ti atoms in anatase nanoparticles.

## Introduction

Nanocrystalline semiconductors coated with photosensitizing agents (usually molecular compounds with low-lying excited electron states) allow for injection of electrons from the photosensitizing molecules into the semiconductor's conduction band under irradiation by visible light. Such a scheme has created new possibilities in a solar cell technology, being an inexpensive alternative to the conventional silicon photovoltaic cells.[1] Dye sensitized solar cells with high photon to current conversion efficiencies and a long life cycle were designed by the Lausanne group on the basis of nanocrystalline anatase ceramics sensitized with a thin layer of ruthenium(II) di- and terpyridine complexes.[2,3]

The efficient Ru-containing photosensitizers, bis(tetrabutylammonium)-*cis*-dithiocyanatobis(2,2′-bipyridine-4-carboxylic,4′-carboxylate)ruthenium(II)$\{(C_4H_9)_4N\}_2$-$[Ru(Hdcbpy)_2(NCS)_2]$, or red dye (**1**),[4] and bis(tetrabutylammonium)trithiocyanato(4,4′,4″-tricarboxy-2,2′:6′,2″-terpyridine)ruthenium(II) $\{(C_4H_9)_4N\}_2[Ru(H_2tcterpy)(NCS)_3]$, or black dye (**2**),[5] have been studied earlier as DMSO solvates by single-crystal X-ray diffraction. Both complexes have planar metal-containing cyclic fragments (metallacycles) and COOH groups in *para*-positions to the coordinated nitrogen atom in the pyridine rings (Figure 1), whose deprotonation at higher pH gives rise to a variety of ionic derivatives. The *para*-COOH or $COO^-$ groups, which are roughly coplanar with the metallacycle, anchor the sensitizer molecules to the $TiO_2$ surface and play a decisive role in the electron transfer through their $\pi^*$-MOs during photoexcitation, thus improving the photochromic properties of the complex.[6]

Thin films of nanocrystalline anatase are usually obtained by the sol−gel technique via a controlled hydrolysis of $TiCl_4$ or titanium alkoxides and a subsequent heating of the solid product at 300−450 °C. A photosensitizer is usually deposited on the nanocrystalline film simply by its exposure to the solutions of the corresponding dyes in organic media. Extensive physicochemical studies of the related materials, including X-ray structural determinations of different photosensitizing complexes,[7−12] XRD[13,14] and electron micros-

* To whom correspondence should be addressed.
[†] Laboratory of Polymer Structural Studies, Institute of Organoelement Compounds, Russian Academy of Sciences.
[‡] Laboratory of Photonics and Interfaces, Institute of Physical Chemistry, Swiss Federal Institute of Technology.
[§] Laboratory of Crystallography, Swiss Federal Institute of Technology.

(1) Hagfeld, A.; Graetzel, M. *Chem. Rev.* **1995**, *95*, 49.
(2) O'Reagan, B.; Graetzel, M. *Nature* **1991**, *353*, 737.
(3) Graetzel, M. *Comments Inorg. Chem.* **1991,** *12*, 93.
(4) Nazeeruddin, M. K.; Kay, A.; Rodicio, I.; Humphry-Baker, R.; Mueller, E.; Liska, P.; Vlachopoulos, N.;Graetzel, M. *J. Am. Chem. Soc.* **1993**, *115*, 6392.
(5) Nazeeruddin, M. K.; Pechy, P.; Graetzel, M. *Chem. Commun.* **1997**, 1705.
(6) Moser, J.; Graetzel, M. *Chem. Phys.* **1993**, *176*, 493.
(7) Heber, R. H.; Nan, G.; Potenza, J. A.; Schugar, H. J.; Bino, A. *Inorg. Chem.* **1989**, *28*, 938.
(8) Shklover, V.; Eremenko, I. L.; Berke, H.; Nesper, R.; Zakeeruddin, S. M.; Nazeeruddin, Md. K.; Graetzel, M. *Inorg. Chim. Acta* **1994**, *219*, 11.
(9) Shklover, V.; Haibach, T.; Bolliger, B.; Hochstrasse, M.; Erbudak, M.; Nissen, H.-U.; Zakeeruddin, S. M.; Nazeeruddin, Md. K.; Graetzel, M. *J. Solid State Chem.* **1997**, *132*, 60.

10.1021/cm020123d CCC: $22.00 
Published on Web 07/26/2002

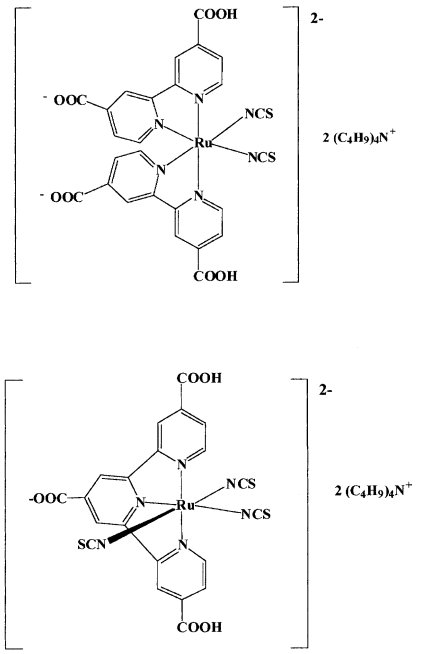


**Figure 1.** Molecular formulas of the red dye **1** (top) and black dye **2** (bottom).

copy[9,10,15] studies of $TiO_2$ nanocrystallites, vibrational spectroscopy of the dyes anchored to $TiO_2$ crystal faces,[12,16,17] and testing the photochemical stability of the resulting materials,[18,19] have been performed during the past decade. Recently, possible modes of dye anchoring to a $TiO_2$ surface have been tested by molecular modeling.[11] However, a thorough characterization of the anatase/sensitizer material in real photovoltaic cells at the atomic level, which is of crucial importance for the elucidation of the electron-transfer mechanism in these systems, is still to be accomplished.

In this paper, we report the characterization of the new photovoltaic element with a complex multilayer structure including a glass support, a thin conducting layer ($SnO_2$), and a layer of sintered nanocrystalline anatase[12] coated with the red dye (**1**), and black dye (**2**), as a sensitizer. The prototypes of solar cells based on the coated nanocrystalline anatase films, as well as their uncoated analogues, have been studied by X-ray diffraction (XRD), X-ray photoelectron spectroscopy (XPS), and X-ray absorption fine structure (XAFS) spectroscopy techniques. Powder XRD patterns for pure dyes **1** and **2** crystallized from EtOH media, as well as the XRD pattern for a single-crystal $TiO_2$ anatase plate, were also measured for reference.

## Experimental Section

**Sample Preparation.** *$TiO_2$ Electrode Preparation.* The $TiO_2$ colloidal paste was prepared using published procedures.[12] The $TiO_2$ paste was deposited onto a sheet glass (Nippon Sheet Glass, Hyogo, Japan, which has been coated with a fluorine-doped stannic oxide layer; sheet resistance of 8−10 $\Omega/cm^2$) using a screen printing technique. The resulting layer was dried in air at 100 °C for 15 min followed by another 15 min at 150 °C. For the final processing, the layers were heated using a titanium hot plate (Bioblock Scientific) to 325 °C at a rate of 30 °C/min and kept at this temperature for 5 min. Then, the temperature was raised to 375 °C at a rate of 10 °C/min and held there for 5 min. Finally, the layers were fired to 450 °C at a rate of 15 °C/min under flowing oxygen and left at this temperature for 20 min before cooling to room temperature.

The 0.05 M titanium tetrachloride solution was prepared in the following manner: first, 2 M titanium tetrachloride solution was prepared by adding directly $TiCl_4$ liquid into a bottle containing ice, which was cooled to −20 °C; then the solution was further diluted to 0.05 M. The heated electrodes were impregnated with a 0.05 M titanium tetrachloride solution in a water saturated desiccator for 30 min at 70 °C and washed with distilled water.

**Uptake of Dyes on Glass Electrodes. Bis(tetrabutylammonium)-cis-dithiocyanatobis(2,2′-bipyridine-4-carboxylic,4′-carboxylate)ruthenium(II) $(TBA)_2[Ru(Hdcbpy)_2(NCS)_2]$, or Red Dye (1), on a $TiO_2$-Covered Plate (plate/1).** Tetrabutylammonium (TBA) salt **1** was obtained as published elsewhere.[4] The dye solutions were prepared in a 1:1 v/v acetonitrile and *tert*-butyl alcohol solvent mixture at a concentration of $5 \times 10^{-4}$ M. The $TiO_2$ electrodes, treated with titanium tetrachloride solution, were heated to 500 °C at a rate of 35 °C/min under $O_2$ atmosphere, left for 10 min at this temperature, and then cooled to ∼100 °C. The hot electrodes were plunged into the dye solution and kept for 12−15 h. The red electrodes were taken out from the solution and then rinsed thoroughly with acetonitrile. The dye-coated electrodes were dried under reduced pressure at 60 °C for 5 h.

**Bis(tetrabutylammonium)trithiocyanato(4,4′,4″-tricarboxy-2,2′:6′,2″-terpyridine)ruthenium(II) $(TBA)_2[Ru(H_2tcterpy)(NCS)_3]$, or Black Dye (2), on a $TiO_2$-Coated Plate (plate/2).** TBA salt **2** was synthesized according to a published method.[12] The dye solutions ($25 \times 10^{-4}$ M) were prepared in ethanol by dissolving the solid at room temperature with magnetic stirring for 2 h. Hot (∼100 °C) $TiO_2$ electrodes, prepared as above, were immersed into the dye solution for 20 h. The black dye-coated electrodes were withdrawn from the solution, rinsed in ethanol, and dried under vacuum for 12 h.

**Scanning Electron Microscopy (SEM).** The samples were examined at 30 kV accelerating voltage in a Hitachi S-900 "in-lens" field-emission scanning electron microscope with a standard Everhard-Thornley

(10) Shklover, V.; Nazeeruddin, M.-K.; Zakeeruddin, S. M.; Barbe, C.; Kay, A.; Haibach, T.; Steurer, W.; Hermann, R.; Nissen, H.-U.; Graetzel, M. *Chem. Mater.* **1997**, *9*, 430.
(11) Shklover, V.; Ovchinnikov, Yu. E.; Braginsky, L. S.; Zakeeruddin, S. M.; Graetzel, M. *Chem. Mater.* **1998**, *10*, 2533.
(12) Nazeeruddin, M. K.; Pechy, P.; Renouard, T.; Zakeeruddin, S. M.; Humphry-Baker, R.; Comte, P.; Liska, P.; Cevey, L.; Costa, E.; Shklover, V.; Spiccia, L.; Deacon, G. B.; Bignozzi, C. A.; Graetzel, M. *J. Am. Chem. Soc.* **2001**, *123*, 1613.
(13) Zhang, H.; Banfield, J. F. *J. Phys. Chem.* **2000**, *104*, 3481.
(14) Wang, Q. J.; Moss, S. C.; Shalz, M. L.; Glaeser, A. M.; Zandbergen, H. W.; Aschack, P. In *Physics and Chemistry of Finite Systems From Clusters to Crystals*; Jena, P., et al., Eds.; Kluwer: The Netherlands, 1992; Vol. II, p 1287.
(15) O'Reagan, M.; Moser, J.; Anderson, M.; Graetzel, M. *J. Phys. Chem.* **1990**, *94*, 8720.
(16) Duffy, D. W.; Dobson, K. D.; Gordon, K. C.; Robinson, B. H.; McQuillan, A. J. *Chem. Phys. Lett.* **1997**, *266*, 45.
(17) Finnie, K. S.; Bartlett, J. R.; Woolfrey, J. L. *Langmuir* **1998**, *14*, 2744.
(18) Gruenwald, R.; Tribusch, H. *J. Phys. Chem. B* **1997**, *101*, 2564.
(19) Kohle, O.; Graetzel, M.; Meyer, A. F.; Meyer, T. B. *Adv. Mater.* **1997**, *9*, 904.

SE detector and a YAG type BSE detector. A sample degradation under an intense electron beam with enlarging of nanoparticle size was observed for coated plate/**1** and plate/**2** samples after the first 10−20 s of exposure.

**X-ray Diffraction.** Polycrystalline **1** and **2** were obtained from the solution of the corresponding complex in an ethanol/water mixture by slow evaporation under air. Precipitation of **1** from acetonitrile media resulted in the amorphous substance without any distinct X-ray reflection pattern, and fast changes of the XRD pattern were observed for **1** prepared from $EtOH/H_2O$ media during the first 30 min. Finely grinded powders of the crystalline **1** and **2** have been placed into sealed boron glass capillaries 0.5 mm in diameter. Powder X-ray diffraction patterns have been obtained at the Swiss-Norwegian BM1B beam line of the European Synchrotron Radiation Facility (Grenoble, France) operating at 7 GeV with an electron current of ∼200 mA. The measurements have been performed on the two-circle diffractometer equipped with four independent Si [111] crystal analyzers and NaI scintillator counters, allowing for simultaneous measurement of four patterns with a $2\theta$ offset of 1.1° and providing the intrinsic angle resolution of 0.01° (at 1 Å). The standard Debye−Scherrer geometry at the wavelength 0.75003 Å obtained by the Si [111] channel-cut monochromator, sample spinning, continuous scanning mode with a $2\theta$ step of 0.01°, and a counting time of about 10 s per point over the total range of 2−40° were applied.

The prototypes of solar cells based on nanocrystalline anatase films coated with dyes **1** and **2** (further referred to as "plate/**1**" and "plate/**2**", respectively), as well as on their uncoated analogue (referred to as "blank plate"), are flat glass plates with the approximate size 20 × 100 $mm^2$. Measurements of their out-of-plane diffraction patterns have been performed at the same beam line with the samples inclined by 0.2−0.3° relative to the incident synchrotron X-ray beam ($\omega$-angle) to minimize the contribution of scattering from the $SnO_2$ conducting layer underneath the nanocrystalline anatase layer and maximize the surface sensitivity. Measurements have been performed with the initially adjusted and then fixed $\omega$ angle, and a continuous scanning of the $2\theta$ angle from 2 to 40° with steps of 0.02° and a counting time of 10 s. A diffraction pattern for a single crystal plate of anatase specifically cut to expose the (101) crystallographic plane (5 × 5 $mm^2$) has been measured under the same conditions for reference.

Standard procedures applied for processing of the powder diffraction patterns included background removal, smoothing, peak search, and intensity normalization. Lattice parameters for dyes **1** and **2** have been obtained by indexing the first 25−30 strong reflections in the experimental powder patterns using the TREOR[20] code followed by refinement of the first-order approximation in the PIRUM[21] program versus all the observed reflections (Table 1).

**X-ray Photoelectron Spectroscopy.** X-ray photoelectron spectra for the solar cell prototypes (both dye-coated and uncoated) have been measured with a Kratos XSAM 800 dual-chamber laboratory XPS spectrometer equipped with a hemispherical electron energy analyzer using Mg Kα radiation ($E = 1253.6$ eV) and energy steps of 0.1 eV. For calibration, the binding energy 285 eV has been assigned to the dominant C 1s contribution (alkyl carbon atoms). The surface compositions of the samples have been calculated from the integral intensities of the XPS lines as described elsewhere.[22]

**Table 1. Unit Cell Parameters of 1 and 2 Obtained by Indexing Their X-ray Powder Diffraction Patterns**

| | **1** | **2** |
|---|---|---|
| radiation source | ESRF, SNBL BM1B | ESRF, SNBL BM1B |
| $\lambda$, Å | 0.75003 | 0.75003 |
| measurement geometry | Debye−Scherrer | Debye−Scherrer |
| lattice | monoclinic P | monoclinic C |
| $a$, Å | 24.800(18) | 29.31(4) |
| $b$, Å | 15.698(6) | 25.99(2) |
| $c$, Å | 7.939(4) | 21.52(4) |
| α, deg | 90 | 90 |
| $\beta$, deg | 92.14(5) | 128.0(1) |
| $\gamma$, deg | 90 | 90 |
| $V$, $Å^3$ | 3088.4 | 12909.0 |
| $2\theta$ range, deg | 3−32 | 2−25 |
| no. of indexed reflections | 61 | 57 |
| $M_{20}$ | 12 | 6 |
| $F_{20}$ | 70 | 43 |
| max. $\lvert 2\theta_{exp} - 2\theta_{calc}\rvert$, deg | 0.022 | 0.024 |

**Ti K-Edge X-ray Absorption Spectroscopy.** Ti K-edge XAFS spectra for solar cell prototypes have been collected at the VEPP-3 storage ring (Budker Institute of Nuclear Physics, Novosibirsk, Russia) operating at 2.0 GeV with the electron current in the range 130−70 mA. Data have been collected in the fluorescence mode with a Si [111] channel-cut monochromator and a scintillator counter with an NaI window, and normalized to $I_0$ measured with an ion chamber. The energy step was ∼0.1 and 1 eV in XANES and EXAFS regions, respectively. Five independent XANES scans with a different dwell time have been taken for each sample to ensure the lack of detector saturation; all experimental patterns were completely consistent. EXAFS spectra for the three samples have been measured up to ∼14 $Å^{-1}$ in the $k$ space. Two-sphere fitting (including single scattering contributions from closest Ti−O and Ti−Ti coordination spheres) has been done using the UWXAFS[23] software with theoretical phases and amplitudes calculated by FEFF.[24]

## Results and Discussion

According to single-crystal X-ray diffraction[25] and powder neutron diffraction data,[26,27] $TiO_2$ anatase forms tetragonal crystals with $a = 3.784$ Å and $c = 9.515$ Å at room temperature, space group $I4_1/amd$, and four formula units per unit cell. The Ti atoms have a distorted octahedral environment of six oxygen atoms with a local $D_{2d}$ symmetry, giving rise to two sym-

(20) Werner, P.-E.; Eriksson, L.; Westdahl, M. *J. Appl. Crystallogr.* **1985**, *18*, 367.
(21) Werner, P.-E. *Ark. Kemi* **1969**, 31, 513.
(22) Pertsin, A. J.; Gorelova, M. M.; Levin, V. Yu.; Makarova, L. I. *J. Appl. Polym. Sci.* **1992**, *45*, 1195.
(23) Newville, M.; Ravel, B.; Haskel, D.; Rehr, J. J.; Stern, E. A.; Yakoby, Y. *Physica B* **1995**, *208−209*, 154.
(24) Rehr, J. J.; Zabinsky, S. I.; Albers, R. S. *Phys. Rev. Lett.* **1992**, *69*, 3397.
(25) Horn, M.; Schweirdtfeger, C. F.; Maegher, E. P. *Z. Kristallogr.* **1972**, *136*, 273.
(26) Burdett, J. K.; Hughbanks, T.; Miller, G. J.; Richardson, J. W.; Smith, J. V. *J. Am. Chem. Soc.* **1987**, *109*, 3693.
(27) Howard, C. J.; Sabine, T. M.; Dickson, F. *Acta Crystallogr.* **1991**, *B47*, 462.

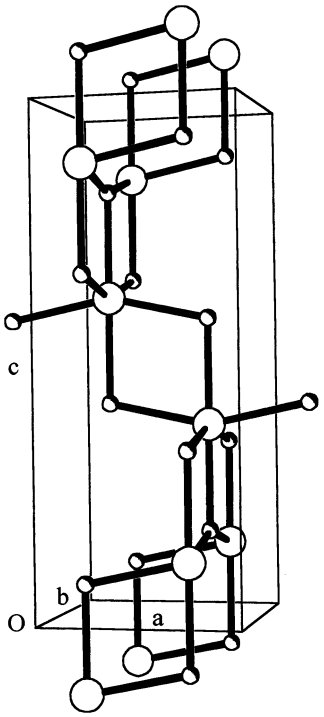


**Figure 2.** Crystal structure of anatase. Large circles denote positions of titanium atoms, and small ones, positions of oxygen atoms.

metrically independent Ti−O bonds of 1.934 Å (four O atoms) and 1.980 Å (two O atoms) in the closest coordination sphere, and four symmetrically equivalent Ti atoms (Ti−Ti 3.039 Å) in the second sphere. Each oxygen atom has a planar trigonal environment of three adjacent Ti atoms (Figure 2).

A number of the experimental XRD and XAFS studies of a local atomic ordering in $TiO_2$ nanoparticles have been recently published.[28−31] Several theoretical simulations of XANES[32−35] gave a reliable assignment of the features in the Ti K pre-edge region. Studies of model organic molecules (viz. ascorbic acid,[30,31] formic acid,[36] and bi-isonicotine acid[37]) anchored to $TiO_2$ crystal faces by XAFS,[30,31] XPS,[36,37] and other methods[31] have been reported. All these data may be used as reference for a structural characterization of the coated and uncoated anathase nanocrystallites in the systems under study.

**Exposed Surface versus Coordination Sites in $TiO_2$ Nanocrystallites.** $TiO_2$ films deposited on the conducting glass in the samples under study consist of anatase nanocrystallites with average diameter 12 nm ± 10% according to electron microscopy. A highly porous $TiO_2$ layer may generally hold the photosensitizing dye in three different ways distinguishable by physical methods: (i) as a separate bulk crystalline or amorphous phase atop the titania layer and within the cavities, (ii) as a monolayer anchored to the surface of nanoparticles, and (iii) as a multilayer epitaxial film on the faces of nanocrystallites. For a dye monolayer suggested in refs 1 and 12, we calculate an idealized "stoichiometry" of the coated particle.

The fraction of surface atoms in these particles may be estimated[28] as $12.5/d$ (where $d$ is the average diameter in angstroms), that gives ∼10% of all atoms in the nanocrystallites lying on their surfaces and coordinated by five O atoms instead of six (neglecting a smaller number of Ti atoms on edges and vertexes). It corresponds to a bulk stoichiometry of approximately $(TiO_{1.97})_nX_m$ (where $n \sim 10^5$, $m \leq n$, and X is any weakly absorbed species such as OH, $H_2O$, organic impurities, and so forth that occupies the sixth coordination site at the surface Ti atoms). Estimating the average nanocrystallite surface area as ∼1000 nm$^2$, from ∼2 nm$^2$ surface area per one doubly anchored molecule of **2**,[11,12] we get 500 photoactive centers per coated particle $(TiO_{1.97})_nL_k$ or only about 1000 Ti atoms per nanocrystallite bonded to dye molecules L (which is ∼1% of their total number in the sample). So more than 80% of the Ti atoms on the particle surface coated with dye monolayer remain sterically screened by dye molecules but uncoordinated. Coating of nanocrystallites by the anchored agent may be therefore considered as a specific case of ligand substitution in the coordination shell of a nanoparticle:

$$(TiO_{1.97})_nX_m + kL \rightarrow (TiO_{1.97})_nL_k + mX$$

favorable from both energy (stronger binding) and entropy viewpoints ($m \gg k$).

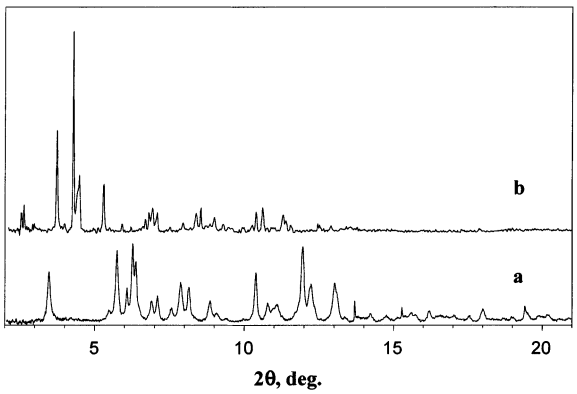


**Figure 3.** Synchrotron X-ray powder diffraction patterns for polycrystalline powder of **1** (a) and **2** (b).

**Powder Diffraction Data for 1 and 2.** The diffraction patterns for crystalline powders of both photosensitizers **1** and **2** are shown in parts a and b, respectively, of Figure 3. Unit cell parameters from their indexing are summarized in Table 1. Though the figures of the merits of the indexing are not very high (the values of $M_{20} > 10$ are usually recommended for an indexing

(28) Chen, L. X.; Raih, T.; Wang, Z.; Thurnauer, M. *J. Phys. Chem. B* **1997**, *101*, 10688.
(29) Luca, V.; Djajanti, S.; Howe, R. F. *J. Phys. Chem. B* **1998**, *102*, 10650.
(30) Chen, L. X.; Raih, T.; Jager, W.; Nedeljkovic, J.; Thurnauer, M. *J. Synchrotron Radiat.* **1999**, *6*, 445.
(31) Raih, T.; Nedeljkovic, J. M.; Chen, L. X.; Poluektov, O.; Thernauer, M. C. *J. Phys. Chem.* **1999**, *103*, 3515.
(32) Parlebas, J. C.; Khan, M. A.; Uozumi, T.; Okada, K.; Kotani, A. *J. Electron Spectrosc. Relat. Phenom.* **1995**, *71*, 117.
(33) Farges, F.; Brown, G. E., Jr.; Rehr, J. J. *Geochim. Cosmochim. Acta* **1996**, *60*, 3023.
(34) Wu, Z. Y.; Ouvrard, G.; Gressier, P.; Natoli, C. R. *Phys. Rev. B* **1997**, *55*, 10382.
(35) Joly, Y.; Cabaret, D.; Renevier, H.; Natoli, C. R. *Phys. Rev. Lett.* **1999**, *82*, 2398.
(36) Wang, L.-Q.; Ferris, K. F.; Shultz, A. N.; Baer, D. R.; Engelhard, M. H. *Surf. Sci.* **1997**, *380*, 352.
(37) Patthey, L.; Rensmo, H.; Persson, P.; Westermark, K.; Vayssieres, L.; Stashans, A.; Petersson, Ao.; Bruehwiler, P. A.; Sieghahn, H.; Lunell, S.; Maortisson, N. *PSI Scientific Report*; Paul Scherrer Institut: Villigen, Switzerland, 1998; Vol. VII, p 53.

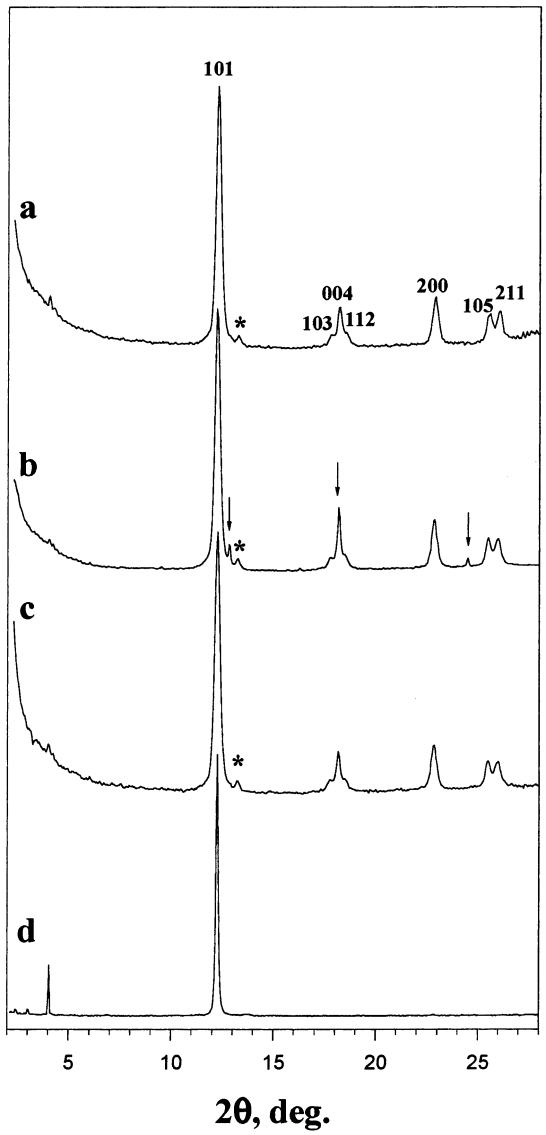


**Figure 4.** Out-of-plane X-ray diffraction ($\omega$ = 0.2−0.5°) patterns for solar cell prototypes: (a) plate/**1**; (b) plate/**2**; (c) uncoated plate; (d) (101) face of anathase single crystal.

solution to be accepted[38]), we consider our indexing reliable, taking into account a large total number of indexed reflections in the big unit cells of low symmetry (monoclinic) and small disagreement between the observed and calculated $2\theta$ positions.

**Out-of-Plane X-ray Diffraction Data for Solar Cell Prototypes.** With a very small incidence angle (0.2−0.5°) of the X-ray beam, a selective diffraction pattern of the upper $TiO_2$ layer of 8−10 $\mu$m thickness can be obtained experimentally almost without contribution from the underneath layer of crystalline $SnO_2$ (Figure 4). A comparison of data for blank and dye-coated $TiO_2$ layers shows the main broadened reflections of anatase with no noticeable difference among the samples. The small peak (marked by the asterisk) near the (101) reflection of anatase corresponds to the strongest (110) reflection of rutile. The same observation, that is, a small admixture of rutile in samples with larger nanocrystallites sintered at ≥400 °C, has been reported earlier by Luca et al.[29] An estimate of the mean diameter of anatase nanocrystallites from line broadening using the Scherrer formula gives $d \sim 12.5$ nm for all plates, in good agreement with SEM data. The weak narrow peaks marked by arrows on the diffractogram of the solar cell prototype coated with **2** correspond to the strongest reflections of the underneath layer of crystalline $SnO_2$. A weak feature at $2\theta \approx 4°$ coincides with the strongest satellite reflection observed under similar conditions for the single-crystal anatase plate with the (101) crystalline plane exposed. Such satellite peaks may correspond to a multiple diffraction phenomena.[39] It is important that neither reflections originated from crystalline powders of **1** and **2** nor a halo at $2\theta \approx 10°$ was observed for plate/**1** and plate/**2** samples. Sedimentation of the dyes or products of their chemical transformations as a separate phase in the cavities between $TiO_2$ nanocrystallites is therefore not consistent with the X-ray diffraction data down to its detection limit. It should be noted, however, that, for a diffraction technique, even with SR sources and small incident angles, this limit is relatively high (∼≤ 1%). For conclusive evidence that a (partial coverage) dye monolayer exists in the coated samples, more experimental data are probably needed.

**Table 2. Binding Energies (BE) and Content (%) of the Surface Elements in the Solar Cell Prototypes from XPS Data**

| spectral feature | plate/**1** | | plate/**2** | | uncoated plate | |
|---|---|---|---|---|---|---|
| | BE, eV | % | BE, eV | % | BE, eV | % |
| C 1s | 284.9 | 22.6 | 284.9 | 22.9 | 284.9 | 16.3 |
| | 286.4 | 8.8 | 286.5 | 8.8 | 286.4 | 7.2 |
| | 288.6 | 3.4 | 288.6 | 2.9 | 288.5 | 2.7 |
| Ru $3d_{5/2}$ | 281.0 | 0.14 | 281.2 | 0.13 | | |
| O 1s | 529.9 | 31.0 | 530.1 | 32.0 | 530.0 | 41.4 |
| | 531.6 | 11.5 | 531.7 | 11.1 | 531.6 | 9.6 |
| | 533.1 | 7.1 | 533.1 | 6.7 | 533.0 | 5.6 |
| Ti $2p_{3/2}$ | 458.6 | 12.7 | 458.9 | 13.0 | 458.7 | 17.0 |
| Ti $2p_{1/2}$ | 464.3 | | 464.5 | | 464.4 | |
| N 1s | 400.0 | 2.2 | 400.0 | 1.9 | | |
| S 2p | 168.8 | 0.6 | 169.0 | 0.6 | | |

**X-ray Photoelectron Spectroscopy Data.** XPS data for plate/**1** and plate/**2** as well as for the uncoated plate allowed us to estimate an amount of Ru species chemisorbed at the surface, to compare it to what is required by the monolayer model. Such elements as C, O, Ti, Ru, N, and S have been included in the analysis. These data (Table 2) show a similar surface chemical composition for both photosensitized plates with a Ti/Ru ratio of ∼100:1, in qualitative agreement with the model of a dye monolayer anchored to a $TiO_2$ nanocrystallite surface (see above). Almost the same Ti/Ru ratio for several samples of plate/**1** and plate/**2**, in accord with XRD data, argues against a deposition of bulk dye "islands" on the surface of $TiO_2$ nanocrystals or in the voids between, since this ratio should be higher and random in such a case. Positions of Ru $3d_{5/2}$ peaks (∼281.1 eV) for the coated samples are close to those typical for $Ru^{2+}$ complexes coordinated to N-ligands.[40] Binding energies for Ti $3p_{3/2}$ (∼458.7 eV) and O 1s (∼530.0 eV) spectral features are in agreement with the values reported earlier for pure anatase.[36] The shape of the Ti $2p_{1/2}/2p_{3/2}$ doublet (Figure 5, top) is virtually

(38) de Wolff, P. M. *J. Appl. Crystallogr.* **1968**, *1*, 108.

(39) Chang, S.-L. *Multiple Diffraction of X-rays in Crystals*; Springer-Verlag: Berlin, 1984.

(40) Battistoni, C.; Furlani, C.; Mattogno, G.; Tom, G. *Inorg. Chim. Acta* **1977**, *21*, L25.

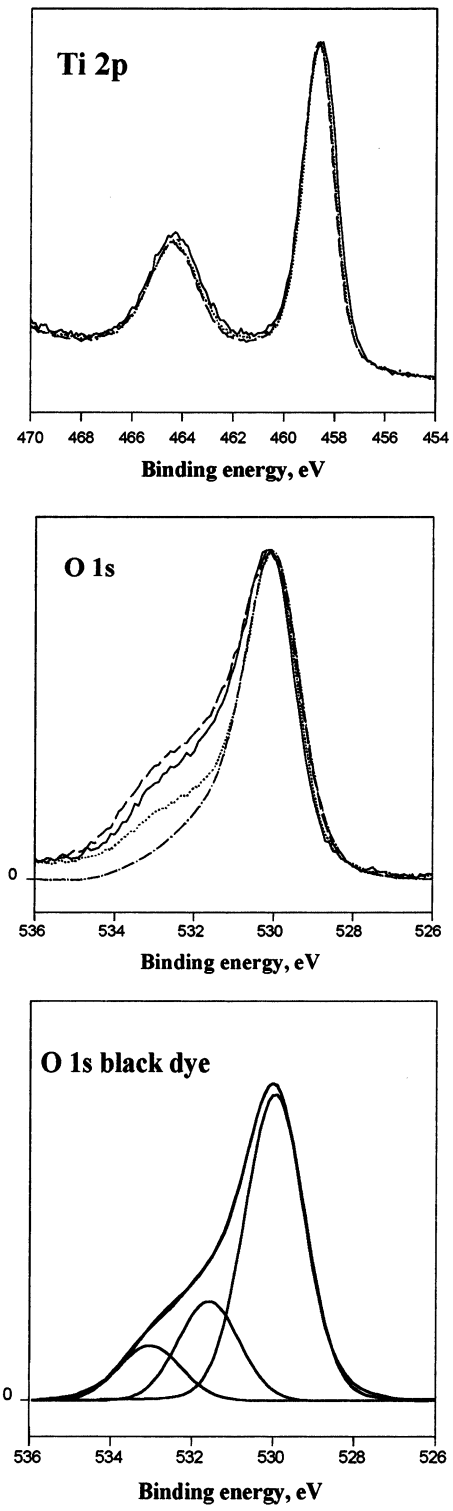


**Figure 5.** Ti 2p (top) and O 1s (middle) XPS core level spectra for solar cell prototypes: plate/**1** (solid line); plate/**2** (dashes); uncoated plate (dots); uncoated plate heated in air (dash−dot). Bottom: a spectral decomposition of the O 1s band into three Gaussian components for the plate/**2** sample.

the same for all three samples, showing that little or no defects emerge during preparation of the coated plates. On the other hand, two additional O 1s components at binding energies of 531.6 and 533.1 eV, corresponding to adsorbed carboxylate species,[37] have been observed for all samples in addition to the major contribution from oxygen atoms of the $TiO_2$ surface (Figure 5, middle). The relative intensities of these two

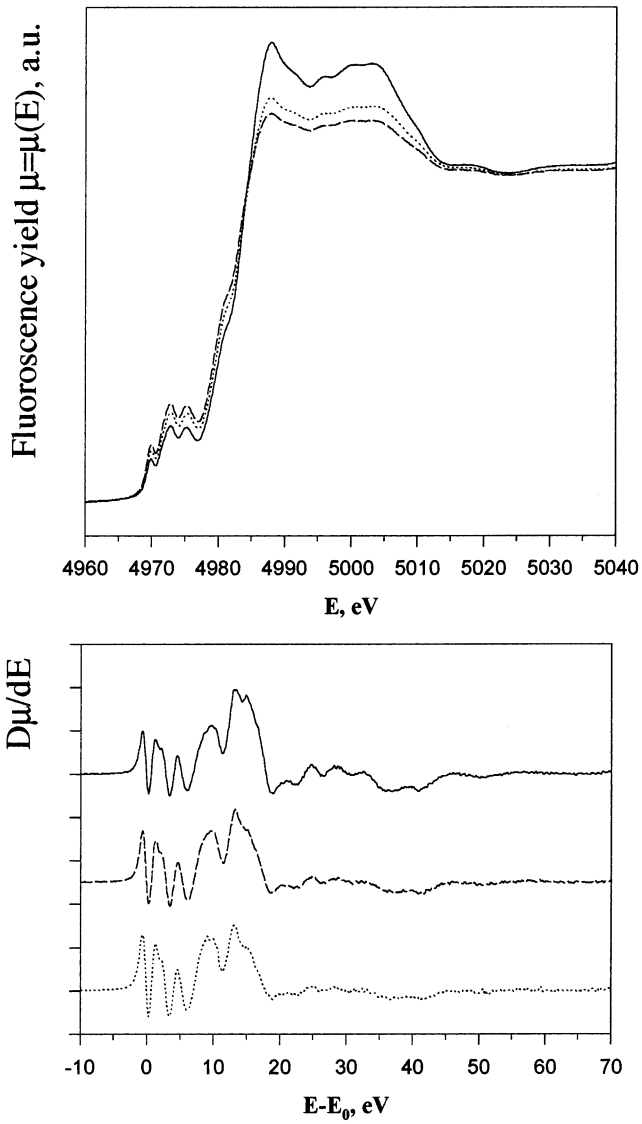


**Figure 6.** Ti K-edge XANES spectra for solar cell prototypes: uncoated plate (solid line); plate/**1** (dashes); (b) plate/**2** (dots). X-ray absorption coefficients measured as a fluorescence yield (top) and its derivative (bottom) are shown.

features for the uncoated $TiO_2$ film are lower when compared to the case of coated plates, and further diminished after heating in air during 4 h at 350 °C (Figure 5, middle, dash−dot curve). These satellite peaks from the "blank" plate are most probably originated from organic complexing agents such as AcOH used in the initial preparation routine of $TiO_2$ colloid (see ref 12 and references therein). Dominance of the $TiO_2$ O 1s peak in coated plate/**1** and plate/**2** gives more evidence that the dyes form a very thin layer around the anatase particles.

**XAFS Study of a Local Ordering in Anatase Nanocrystallite Films at the Ti K-Edge.** Ti K-edge XANES patterns for the coated nanocrystalline films on plate/**1** and plate/**2**, as well as for the uncoated $TiO_2$ film on the blank plate, are shown in Figure 6. Near-edge features in anatase are marked according to current notation.[29−31,34] From most theoretical results, the pre-edge triplet ($A_1$, $A_{2,3}$, B) corresponds to quadrupole ($A_1$) and dipole ($A_3$, B) 1s−3d transitions, due to a distortion of the centrosymmetric octahedral environment (see Figure 2), with the participation of valence p-AOs of

**Table 3. Local Order Parameters in Nanocrystalline Anatase Powders with Different Particle Sizes from XAFS Data**

| | | Ti−O | | | Ti−Ti | | | |
|---|---|---|---|---|---|---|---|---|
| sample | *d*, nm | *R*, Å | *N* | $\sigma^2$, Å$^2$ | *R*, Å | *N* | $\sigma^2$, Å$^2$ | ref |
| anatase | 1.9 | 1.96 | 4.6 | 0.0004 | | | | 30 |
| anatase modified with ascorbic acid | 1.9 | 1.94 | 5.8 | 0.012 | | | | 30 |
| anatase | 3.0 | 1.99 | 4.0 | 0.003 | | | | 28 |
| anatase | 3.8 | 1.95 | 4.9 | 0.002 | 3.07 | 2.8 | 0.004 | 29 |
| anatase | 5.0 | 1.94 | 5.0 | 0.003 | | | | 28 |
| anatase | 5.1 | 1.94 | 5.9 | 0.002 | 3.05 | 5.1 | 0.006 | 29 |
| anatase | 6.5 | 1.94 | 6.4 | 0.003 | 3.05 | 3.5 | 0.003 | 29 |
| anatase | 11.0 | 1.94 | 5.3 | 0.005 | 3.05 | 1.9 | 0.002 | 29 |
| uncoated solar cell prototype | 12.5 | 1.96 | 4.6 | 0.005 | 3.04 | 2.7 | 0.005 | *a* |
| red dye-coated solar cell prototype | 12.5 | 1.97 | 2.8 | 0.004 | 3.07 | 1.4 | 0.004 | *a* |
| black dye-coated solar cell prototype | 12.5 | 1.97 | 3.5 | 0.004 | 3.07 | 1.3 | 0.002 | *a* |
| anatase | 20 | 1.92 | 6.4 | 0.010 | 3.09 | 4.6 | 0.006 | 28 |
| anatase | 50 | 1.96 | 6.0 | 0.0004 | | | | 30 |
| anatase | 60 | 1.94 | 6.0 | 0.001 | 3.05 | 4.0 | 0.002 | 29 |

[a] This work.

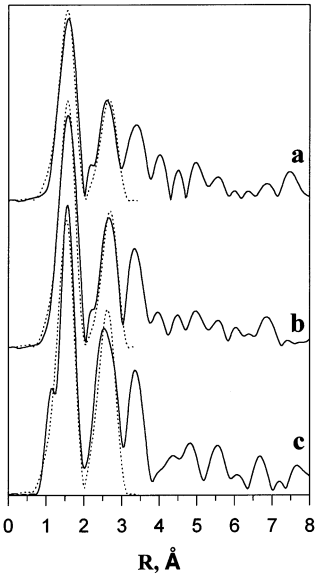


**Figure 7.** Fourier transform magnitudes of EXAFS spectra for solar cell prototypes: (a) plate/**1**; (b) plate/**2**; (c) uncoated plate; (solid line) experimental; (dots) two-sphere fitting.

titanium and oxygen atoms.[32,36] A weak splitting of the $A_{2,3}$ peak, revealed by the $d\mu/dE$ plot at the bottom of Figure 6, was attributed either to a further splitting of the degenerated electronic states of the octahedral crystal field in the actual $D_{2d}$ point symmetry[34] or to pentacoordinated surface Ti atoms;[29,30] the latter viewpoint seems to us most adequate. The middle-edge feature C is believed to correspond to the allowed 1s−4p transition, whereas the"white line" feature D is most obviously due to promotion of a photoelectron onto higher lying vacant np orbitals of Ti and Ti−O antibonding levels in the coordination environment of Ti.[32−35]

In agreement with the small number of coordinated Ti atoms in the model of the dye monolayer, XANES patterns are generally similar for all the samples studied. Two small differences between the coated and "blank" nanocrystallite thin films are (a) a slight enhancement of the pre-edge features and (b) a substantial damping of the "white line" D peak together with the post-edge features, in the coated samples plate/**1** and plate/**2** as compared with the blank plate. A weak low-energy shoulder $A_2$ (which is most pronounced in smaller nanocrystallites of dimensions 2−5 nm[28−31] and was reported to diminish in 2 nm anatase crystallites covered with ascorbic acid[30,31]) shows no change upon coating with dyes in our samples because of a relatively small fraction of surface atoms in 12 nm nanocrystallites (∼10%) and the even smaller fraction of coordinated Ti centers on their surface.

The uniform enhancement of the pre-edge peaks, which are forbidden in the centrosymmetric octahedral environment, may correspond to higher distortions of a local Ti coordination in the coated samples. The other hypothetical origins of these features, viz. detector oversaturation and nonlinearity, may be ruled out by the similarity of XANES patterns collected at different count rates (see Experimental Section), whereas a self-absorption of Ti Kα X-ray fluorescence by a very thin Ru-containing dye layer, rather transparent to photoelectrons (see Figure 5), seems to be improbable.

The post-edge patterns of anatase have not yet been a subject of a rigorous theoretical treatment. From a very general viewpoint, they represent a set of quasi-stationary states, which may qualitatively correspond to a photoelectron multiple scattering.[41] Smearing of these post-edge features in coated nanocrystallites is most probably due to disordering in the local atomic environment, which is in agreement with the enhanced pre-edge peaks.

Ti K-edge EXAFS data support the higher disorder of a local atomic environment in coated anatase nanocrystallites. Notable damping of EXAFS oscillations in the covered $TiO_2$ (plate/**1** and plate/**2**) reduces the peaks of coordination spheres in the FT magnitude plot (Figure 7). Interatomic distances from two-sphere fitting for our glass/$TiO_2$ samples agree with the published data (Table 3), whereas the coordination numbers $N_{Ti-O}$ and $N_{Ti-Ti}$ for the coated plates are drastically diminished in comparison with those for the "blank" one. Since the fraction of coordinated surface Ti atoms in the total number of Ti atoms in nanocrystallite is small (see above), a damping of the coordination spheres reveals some local atomic disordering in the bulk of nanocrystallites upon coating. Noteworthy, such a local disordering does not affect the long-range order in the nanocrystallites under study, since the coherence length is virtually the same in coated and uncoated samples according to XRD data (Figure 4).

(41) Teo, B. K. *EXAFS: basic principles and data analysis*; Springer-Verlag: Berlin, 1985.

In a remarkable paper by Rajh et al.,[31] drastic changes of electrophysical properties of smaller titania nanoparticles, viz. a red shift of the light absorption onset for ~1.6 eV due to a coating of a strongly binding colorless surface modifier (ascorbic acid), were reported. These results, supported by XAFS, FTIR, and ESR data, display the fact that small anatase nanocrystallite with $\sim 10^4$ atoms may act as a unified atomic and electronic system, whose measurable characteristics display different changes when the surface is coated by weakly binding and strongly binding molecules. In agreement with these results, our data obtained for the photosensitized and blank solar cell prototypes show that the local atomic ordering in larger anatase nanocrystallites is sensitive to the alteration of the nanoparticles' shell.

$TiO_2$ nanocrystallites surrounded by a relatively small number (few hundreds) of the anchoring agents may therefore be considered as big coordinated nanocluster centers, whose electronic structure may be affected not only by charge-separation[1−3] and charge-transfer properties[31] of the coating "ligands" but also by a ligand-induced local atomic disordering. Experimental studies of the atomic order within the anchored dye layer using STM and grazing incidence diffraction of **1** and **2** deposited on a clean face of an anatase single crystal will be carried out in the near future.

## Conclusions

(1) Powder XRD data for pure photosensitizers **1** (red dye) and **2** (black dye) recrystallized from a $EtOH/H_2O$ mixture show formation of new crystalline solvates whose unit cell parameters were obtained.

(2) X-ray diffraction patterns from a surface layer for solar cell prototypes with $TiO_2$ nanocrystalline film coated with **1** and **2**, as well as for the uncoated film, show broadened anatase reflections corresponding to the average nanocrystallite dimensions of ~12.5 nm. No evidence of a separated bulk dye phase were obtained above the sensitivity limit of this technique, though a presence of small quantities of a poorly ordered dye still cannot be ruled out.

(3) XPS data for the same coated and uncoated samples allow us to determine the stoichiometry of the anchored photosensitizer (Ru per Ti) as ~1:100 and show a dominance of the anatase O 1s band that agrees with a model of a monomolecular coating.

(4) Ti K-edge XAFS data revealed stronger local atomic disordering in the samples coated by dye molecules in comparison with the blank ones.

**Acknowledgment.** The authors are grateful to the Swiss National Science Foundation for financial support through the SCOPES 2000-2003 program, project 7SUPJ062151.00/1. Yu.L.S. and Y.V.Z. are also indebted to the Russian Foundation for Basic Research (Grant 99-03-32810). We are very grateful to Dr. Hermann Emerich (SNBL, ESRF, Grenoble) and Dr. Nikolai Bausk (Institute of Inorganic Chemistry, Novosibirsk) for highly professional guidance in synchrotron XRD and fluorescence XAFS measurements, respectively, and to Ilya Volkov (Institute of Organoelement Compounds R.A.S.) for a collection of some XPS data. We are thankful to the reviewers for many stimulating comments that were a great help in clarifying our discussion.

**Supporting Information Available:** A list of indexed XRD reflections for **1** and **2** and discrepancies between experimental and calculated positions in the PIRUM output format (ASCII). This material is available free of charge via the Internet at http://pubs.acs.org.

CM020123D